

Doping effect on the structure and physical properties of quasi-one-dimensional compounds $Ba_9Co_3(Se_{1-x}S_x)_{15}$ (x = 0-0.2)

Lei Duan(段磊), Xian-Cheng Wang(望贤成), Jun Zhang(张俊), Jian-Fa Zhao(赵建发), Wen-Min Li(李文敏), Li-Peng Cao(曹立朋), Zhi-Wei Zhao(赵志伟), Changjiang Xiao(肖长江), Ying Ren(任瑛), Shun Wang(王顺), Jinlong Zhu(朱金龙), and Chang-Qing Jin(靳常青)

Citation: Chin. Phys. B, 2021, 30 (**10**): 106101. DOI: 10.1088/1674-1056/ac1f03
Journal homepage: http://cpb.iphy.ac.cn; http://iopscience.iop.org/cpb

What follows is a list of articles you may be interested in

Improved carrier transport in Mn:ZnSe quantum dots sensitized La-doped nano-TiO_2 thin film

Shao Li(李绍), Gang Li(李刚), Li-Shuang Yang(杨丽爽), Kui-Ying Li(李葵英)
Chin. Phys. B, 2020, 29 (**4**): 046104. DOI: 10.1088/1674-1056/ab7742

First-principles investigation on N/C co-doped CeO_2

Rong-Kang Ren(任荣康), Ming-Ju Zhang(张明举), Jian Peng(彭健), Meng Niu(牛猛), Jian-Ning Li(李健宁), Shu-Kai Zheng(郑树凯)
Chin. Phys. B, 2017, 26 (**3**): 036102. DOI: 10.1088/1674-1056/26/3/036102

Influence of nitrogen and magnesium doping on the properties of ZnO films

Dong-hua Li(李东华), Hui-Qiong Wang(王惠琼), Hua Zhou(周华), Ya-Ping Li(李亚平), Zheng Huang(黄政), Jin-Cheng Zheng(郑金成), Jia-Ou Wang(王嘉鸥), Hai-jie Qian(钱海杰), Kurash Ibrahim(奎热西), Xiaohang Chen(陈晓航), Huahan Zhan(詹华瀚), Yinghui Zhou(周颖慧), Junyong Kang(康俊勇)
Chin. Phys. B, 2016, 25 (**7**): 076105. DOI: 10.1088/1674-1056/25/7/076105

Structural and magnetic properties of $BiFe_{1-x}Cr_xO_3$ synthesized samples

S. S. Arafat
Chin. Phys. B, 2014, 23 (**6**): 066101. DOI: 10.1088/1674-1056/23/6/066101

Doping effects on structural and magnetic evolutions of orthoferrite $SmFe_{(1-x)}Al_xO_3$

Li Na-Na, Li Hui, Tang Rui-Lian, Han Dan-Dan, Zhao Yong-Sheng, Gao Wei, Zhu Pin-Wen, Wang Xin
Chin. Phys. B, 2014, 23 (**4**): 046105. DOI: 10.1088/1674-1056/23/4/046105

Doping effect on the structure and physical properties of quasi-one-dimensional compounds $Ba_9Co_3(Se_{1-x}S_x)_{15}$ ($x = 0$–0.2)*

Lei Duan(段磊)[1], Xian-Cheng Wang(望贤成)[2,3,†], Jun Zhang(张俊)[2,3], Jian-Fa Zhao(赵建发)[2,3], Wen-Min Li(李文敏)[2,3], Li-Peng Cao(曹立朋)[2,3], Zhi-Wei Zhao(赵志伟)[1], Changjiang Xiao(肖长江)[1], Ying Ren(任瑛)[1], Shun Wang(王顺)[1], Jinlong Zhu(朱金龙)[4,‡], and Chang-Qing Jin(靳常青)[2,3,5,§]

[1] *School of Materials Science and Engineering, Henan University of Technology, Zhengzhou* 450007, *China*
[2] *Beijing National Laboratory for Condensed Matter Physics, Institute of Physics, Chinese Academy of Sciences, Beijing* 100190, *China*
[3] *School of Physics, University of Chinese Academy of Sciences, Beijing* 100190, *China*
[4] *Department of Physics, Southern University of Science and Technology (SUSTech), Shenzhen* 518055, *China*
[5] *Materials Research Laboratory at Songshan Lake, Dongguan* 523808, *China*

(Received 7 June 2021; revised manuscript received 30 July 2021; accepted manuscript online 19 August 2021)

A series of samples of $Ba_9Co_3(Se_{1-x}S_x)_{15}$ ($x = 0$, 0.05, 0.1, 0.15, 0.2) with quasi-one-dimensional (1D) structure were successfully synthesized under high-temperature and high-pressure conditions. The influence of partial substitution of S for Se on the structure, electronic transport, and magnetic properties of $Ba_9Co_3(Se_{1-x}S_x)_{15}$ has been investigated in detail. The x-ray diffraction data shows that the lattice constant decreases linearly with increasing S-doping level, which follows the Vegrad's law. The doped S atoms preferentially occupy the site of Se atoms in $CoSe_6$ octahedron. Physical properties measurements indicate that all the samples of $Ba_9Co_3(Se_{1-x}S_x)_{15}$ are semiconducting and display spin glass behavior. As the replacement of Se by smaller size S, although the inter-chain distance decreases, the electronic hopping between $CoSe/S_6$ chains is weakened and leads to an increase of band gap from 0.75 eV to 0.86 eV, since the S-3p electrons are more localized than Se-4p ones. $Ba_9Co_3(Se_{1-x}S_x)_{15}$ exhibits 1D conducting chain characteristic.

Keywords: doping effect, one-dimensional chain, spin glass, high-pressure synthesis

PACS: 61.05.cp, 75.50.Lk, 61.66.Fn, 61.82.Fk **DOI:** 10.1088/1674-1056/ac1f03

1. Introduction

Quasi-one-dimensional (1D) systems have attracted intense attention because of their various exotic physical properties such as superconductivity,[1–4] Bose–Einstein condensation,[5] and quantum phase transition.[6–8] Recently, a series of trimerized compounds $Ba_9M_3X_{15}$ (M = V, Fe, Co, Sn; X = S, Se, Te) with quasi-1D structure have been synthesized and studied actively.[9–13] These compounds crystalize into a hexagonal structure with the space group of P-6c2, as schematically demonstrated in Fig. 1. The face-sharing MX_6 octahedrons stack along the c axis to form $–M_2–M_1–M_2–$ one-dimensional chains. These chains are triangularly arranged in the ab-plane and separated by Ba atoms. Besides these MX_6 chains, there exist X-chains located at the center of the triangular lattice. The distance of the nearest neighbor of MX_6 chains is very large, given by the lattice constant a about 9 Å, displaying strongly 1D crystal structure characteristic. These compounds present 1D conducting chain characteristic and complex magnetic ground states owing to their unique structure. For example, $Ba_9Fe_3Te_{15}$ exhibits a spin-glass behavior with freezing temperature at $T_f \sim 6.0$ K and a hump with the maximum susceptibility at 190 K.[10] $Ba_9V_3Se_{15}$ undergoes a ferrimagnetic transition at 2.5 K and presents 1D ferromagnetic chains properties, i.e., $T^{1/2}$ magnetic specific heat above the ordered temperature.[12] Substitution of V by Co, trimerized $Ba_9Co_3Se_{15}$ hosts a spin glass transition at ~ 3 K, which mainly arises from the magnetic frustration due to the geometrically frustrated triangular lattice.[9]

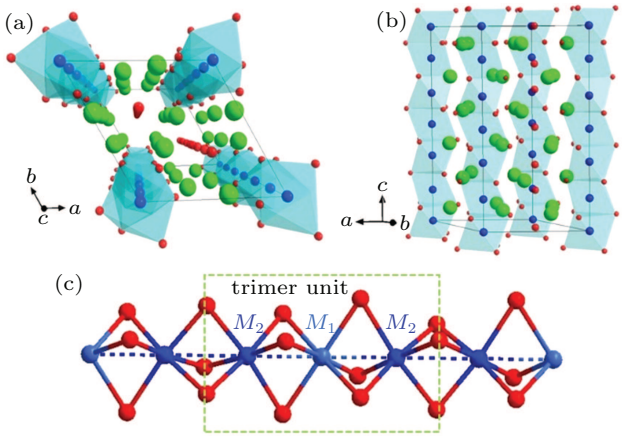


Fig. . Schematic diagram of the $Ba_9M_3X_{15}$ (M = V, Fe, Co, Sn; X = S, Se, Te) in ab-plane (a) and along the c axis (b), and individual MX_6 chain (c). Green balls are Ba atoms, deep bule balls are M atoms, and red balls are X atoms.

*Project supported by the Doctoral Fund of Henan University of Technology (Grant No. 2020BS029), the National Key R&D Program of China (Grant Nos. 2018YFA0305700 and 2017YFA0302900), the National Natural Science Foundation of China (Grant Nos. 11974410 and 11820101003), and the Stable Support Plan Program of Shenzhen Natural Science Fund (Grant No. 20200925152415003).

†Corresponding author. E-mail: wangxiancheng@iphy.ac.cn
‡Corresponding author. E-mail: zhujl@sustech.edu.cn
§Corresponding author. E-mail: jin@iphy.ac.cn

© 2021 Chinese Physical Society and IOP Publishing Ltd

For a quasi-1D system, the interaction and electronic hopping between the adjacent chains has an important influence on the electronic transport and magnetic properties.[14,15] Chemical doping can effectively shorten the distance and increase the orbital overlap between the atoms, thereby controlling the crystal structure, electronic structure, and even degrees of freedom of orbital and spin.[16] Hence, chemical doping provides an effective way to tune the interchain electronic hopping and spin interaction, and thus helps us to study and regulate the physical properties of quasi-one-dimensional materials. For example, quasi-1D $BaVS_3$ displays an insulator behavior with incommensurate anti-ferromagnetic order transition,[17] and the substitution of Se in S site enhances the electronic hoping among chains and then results in a metal to insulator transition.[18] In the series of $Ba_9Fe_3X_{15}$ (X = S, Se, Te), the variation of anion from S to Te leads to the enhancement of interchain interaction and electronic hopping, which have a significant effect on their transport and magnetic properties.[10,19,20] Besides a spin glass transition at $\sim$ 3 K, iso-structure $Ba_9Co_3Se_{15}$ also possesses a 1D conducting characteristic.[9] It is interesting to study the effect of chemical doping on the physical properties of $Ba_9Co_3Se_{15}$. Here, we report on the synthesis of $Ba_9Co_3(Se_{1-x}S_x)_{15}$ ($x = 0$, 0.05, 0.1, 0.15, 0.2) and the influence of S substitution on the crystal structure, electrical transport, and magnetic properties of recently discovered $Ba_9Co_3Se_{15}$.

2. Experimental methods

Commercially available lumps of Ba (Alfa, immersed in oil, $>$ 99.2% pure) and powders of Co (Alfa, 99.995% pure), Se (Alfa, 99.999% pure), and S (Alfa, 99.999% pure) were used as starting materials for sample synthesis. The precursors BaSe were prepared by the reaction of the Ba blocks and Se powders in an alumina crucible sealed in an evacuated quartz tube at 700 °C for 20 h. The obtained BaSe powder, Se, S, and Co powder were mixed according to the elemental ratio of stoichiometric $Ba_9Co_3(Se_{1-x}S_x)_{15}$ ($x = 0$, 0.05, 0.1, 0.15, 0.2), and pressed into a pellet with a diameter of 6 mm, and then loaded to a cubic anvil high-pressure apparatus under 5 GPa and 1000 °C for 30 min, of which the details have been reported in Refs. [21,22]. After the high-pressure and high-temperature process, the black polycrystalline samples were obtained.

Room temperature powder x-ray diffraction (XRD) was conducted on a Huber diffractometer with Cu K_α radiation ($\lambda = 1.54060$ Å). The XRD data were collected with a scanning rate of 1 °/min and a scanning step of 0.02°. The Rietveld refinements on the diffraction patterns were performed using GSAS software packages. The dc magnetization measurements were carried out using a superconducting quantum interference device (SQUID) in the temperature range of 2–300 K under the field of 0.1 T. The temperature dependence of electrical resistivity $\rho(T)$ in the temperature range of 2–300 K was measured by four-probe electrical conductivity methods in a physical property measuring system (PPMS). The ac magnetic susceptibility was also measured by PPMS at different frequencies ranging from 133 Hz to 6333 Hz.

3. Results and discussion

Polycrystalline samples of $Ba_9Co_3(Se_{1-x}S_x)_{15}$ ($x = 0$, 0.05, 0.1, 0.15, 0.2) were synthesized under high pressure and high temperature conditions. Powder x-ray diffraction patterns measured at room temperature for all the samples with nominal composition $Ba_9Co_3(Se_{1-x}S_x)_{15}$ ($x = 0$, 0.05, 0.1, 0.15, 0.2) are shown in Fig. 2(a). It can be seen that all these diffraction patterns can be indexed into a hexagonal structure with the space group P-6c2. The enlarged views are shown in Fig. 2(b).

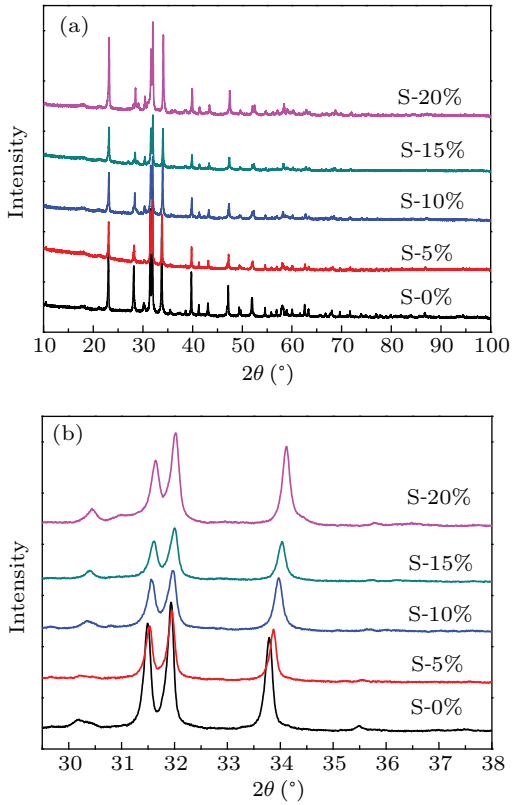


Fig. 2. (a) XRD patterns of $Ba_9Co_3(Se_{1-x}S_x)_{15}$ ($x = 0$, 0.05, 0.1, 0.15, 0.2) measured at room temperature. (b) The enlarged view between 29° and 38°.

We observed that the peaks shift monotonously towards a high-angle direction with the increase of content in the S dopants. This result demonstrates that the S atoms are successfully doped into $Ba_9Co_3Se_{15}$ and implies that the lattice shrinks with S doping. Then the structure of $Ba_9Co_3Se_{15}$ was adopted as the initial model to carry out the refinements for the XRD data of $Ba_9Co_3(Se_{1-x}S_x)_{15}$ ($x = 0$, 0.05, 0.1, 0.15, 0.2). The refinement for the XRD of $Ba_9Co_3(Se_{1-x}S_x)_{15}$ with

$x = 0.2$ is shown in Fig. 3(a), and the others are displayed in Figs. S1(a)–S1(d). The lattice parameters a and c can be obtained from the refinements. The obtained lattice constants $a = 9.6994(1)$ Å and $c = 18.9842(3)$ Å of $Ba_9Co_3Se_{15}$ agree with those reported in the previous work.[9] The doping dependence of the lattice parameters is shown in Fig. 3(b).

These lattice constants decrease linearly as the doping level x increases as expected due to the smaller ionic radius of S compared to Se, implying that the solid solutions follow Vegrad's law. The summary of the crystallographic data for $Ba_9Co_3(Se_{1-x}S_x)_{15}$ with $x = 0.2$ is obtained and listed in Table 1, and the others are exhibited in Tables S1–S4. For the compound $Ba_9Co_3Se_{15}$, there are six atomic sites for Se, two sites in the $CoSe_6$ chain and the other four sites in the Se-chain. From Table 1, we can see that when S is doped, S ions prefers to first occupy the atomic sites of Se/S in the $CoSe/S_6$ octahedral chain. The situation is the same for the other S-doping levels. Within the S-doping level less than 20%, the occupation of S on the Se/S sites in the Se/S_6 chain is zero. When increasing the S-doping level, the occupation of S on Se sites in $CoSe_6$ chain increases gradually, as shown in Table 2. The similar site-selected doping phenomena have also been observed in the $Ba_9Sn_3(Se_xTe_{1-x})_{15}$ series.[13]

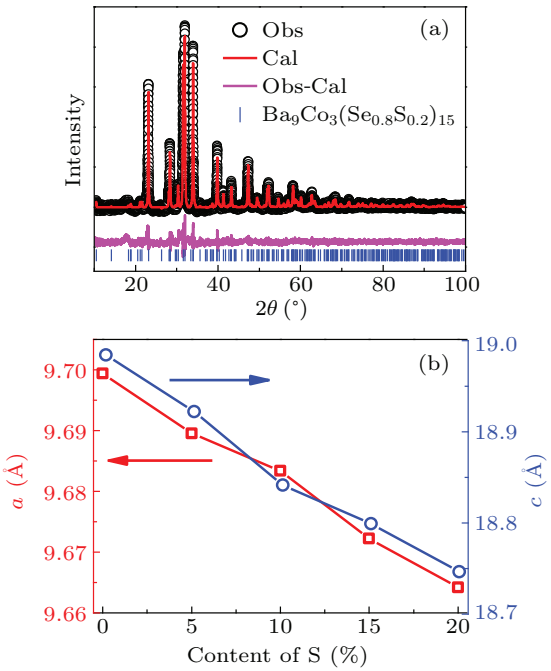


Fig. 3. (a) XRD patterns and the refinements with a hexagonal structure and the space group of P-6c2 for $Ba_9Co_3(Se_{1-x}S_x)_{15}$ with $x = 0.2$. (b) Variation of the lattice parameter as a function of S content.

Table 1. Crystallographic data for $Ba_9Co_3(Se_{0.80}S_{0.20})_{15}$.

Coupound:			$Ba_9Co_3(Se_{0.80}S_{0.20})_{15}$				
Space group: P-6c2 (No. 188); hexagonal; $a = b = 9.6642(4)$ Å, $c = 18.7464(8)$ Å; $V = 1516.28(1)$ Å^3, $Z = 2$; $\chi^2 = 3.4$, $R_{wp} = 5.35\%$, $R_p = 3.74\%$							
Atom	Label	Wyck	x/a	y/b	z/c	SOF	U (Å)
Ba	Ba1	12l	–0.0059(9)	0.3700(9)	0.0804(7)	1	0.024(9)
Ba	Ba2	6k	0.3671(5)	0.3547(3)	1/4	1	0.023(6)
Co	Co1	2a	0	0	0	1	0.019(3)
Co	Co2	4g	0	0	0.1494(6)	1	0.026(4)
Se	Se1	12l	0.2439(9)	0.2575(3)	0.0844(4)	0.6843	0.017(8)
S	S1	12l	0.2439(9)	0.2575(3)	0.0844(4)	0.3157	0.019(4)
Se	Se2	6k	–0.0528(0)	0.1719(2)	1/4	0.6603	0.010(9)
S	S2	6k	–0.0528(0)	0.1719(2)	1/4	0.3397	0.028(1)
Se	Se3	2c	1/3	2/3	0	1	0.018(7)
S	S3	2c	1/3	2/3	0	0	
Se	Se4	4h	1/3	2/3	0.1774(0)	1	0.024(3)
S	S4	4h	1/3	2/3	0.1774(0)	0	
Se	Se5	4i	2/3	1/3	0.1496(5)	1	0.019(0)
S	S5	4i	2/3	1/3	0.1496(5)	0	
Se	Se6	4i	2/3	1/3	0.0121(8)	0.5	0.021(5)
S	S6	4i	2/3	1/3	0.0121(8)	0	

Table 2. The occupation of S atoms on Se sites for $Ba_9Co_3(Se_{1-x}S_x)_{15}$.

x	0	0.05	0.10	0.15	0.20
Se1	1	0.9173	0.8431	0.7639	0.6843
S1	0	0.0827	0.1569	0.2361	0.3157
Se2	1	0.9293	0.8186	0.7380	0.6603
S2	0	0.0707	0.1814	0.2620	0.3397

Table 3 shows some selected important distances and angles of $Ba_9Co_3(Se_{1-x}S_x)_{15}$. In a trimer unit of $Ba_9Co_3(Se_{1-x}S_x)_{15}$, there are two Co atoms on the Co2 site and one on the Co1 site, as shown in Fig. 1(c). Upon increasing the S content, the distance of the adjacent Co1–Co2 (d_{12}) decreases, while the distance of the adjacent Co2–Co2 (d_{22}) increases. The radio of $(|d_{22} - d_{12}| : |d_{22} + d_{12}|)$ can well show the degree of trimerization.[11] According to the distances of adjacent Co1–Co2 and Co2–Co2 in Table 3, we can obtain that the trimerization degree increases continuously from 7.4 % for $x = 0$ to 14.7% for $x = 0.20$, which indicates that substitution of S tends to the formation of trimerization in this system. The bond angle of Se(S)1–Co1–Se(S)1 of $Ba_9Co_3(Se_{1-x}S_x)_{15}$ is also shown in Table 3. It can be observed that all the angles deviate from the value of 180° in a regular octahedron, which suggests that the $CoSe(S)_6$ oc-

tahedrons are slightly compressed along the c axis. The averaged intra-chain distance d_{intra} of Co–Co can be calculated using the lattice constant c divided by six and the inter-chain distance d_{inter} is equal to the lattice constant a, as shown in Fig. 4. We can obviously observe that with the replacement of S, the averaged intra-chain distance d_{intra} and inter-chain distance d_{inter} both gradually decrease as expected. For a quasi-one-dimensional system, the d_{intra} and d_{inter} have a key influence on the physical properties. Hence the replacement of S on Se should affect the properties of $Ba_9Co_3(Se_{1-x}S_x)_{15}$, as we will discuss below.

Table 3. Selected distances (Å) between adjacent atoms and angles (°).

x	0	0.05	0.10	0.15	0.20
Co1–Co2 (d_{12})	3.0033(1)	2.9521(3)	2.8767(1)	2.8233(2)	2.8026(4)
Co2–Co2 (d_{22})	3.4855(3)	3.5570(2)	3.6660(2)	3.7531(1)	3.7680(2)
Se(S)1–Co1–Se(S)1	176.4(1)	176.0(7)	175.1(2)	175.0(6)	175.5(3)

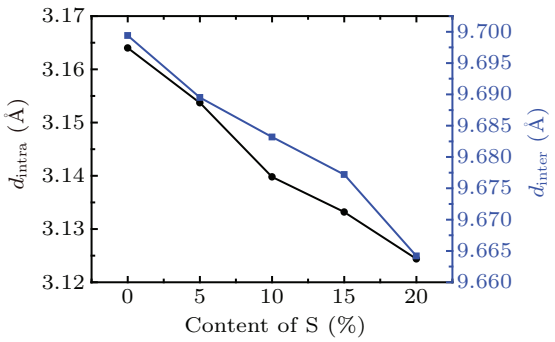


Fig. 4. The S doping dependence of the d_{intra} and d_{inter}. d_{intra} denotes the averaged intra-chain distance of Co–Co; while d_{inter} denotes the inter-chain distance.

The dc magnetic susceptibility measurement as a function of temperature for $Ba_9Co_3(Se_{1-x}S_x)_{15}$ samples was carried out with an applied field of 1000 Oe in both zero-field-cooled (ZFC) and field-cooled (FC) modes to explore the doping effect on the magnetic properties of $Ba_9Co_3(Se_{1-x}S_x)_{15}$. The magnetic susceptibility curves of $Ba_9Co_3(Se_{1-x}S_x)_{15}$ samples in the temperature range 2–60 K are shown in Fig. 5(a). It is seen that the ZFC and FC curves of $Ba_9Co_3Se_{15}$ are overlapped in high temperature region and then begin to bifurcate at about 5 K, which demonstrates a λ-shape agreed with the previous report. Meanwhile, the spin glass behavior of $Ba_9Co_3Se_{15}$ with frozen temperature T_f about 3 K is confirmed by ac susceptibility curves.[9] The temperature dependence of magnetization of all doped samples also exhibits clear cusps at low temperature, which is similar to that of $Ba_9Co_3Se_{15}$ (shown in Fig. 5(a)), suggesting that all the doped samples also display a spin-glass-like behavior like $Ba_9Co_3Se_{15}$. To verify the spin glass feature, we measured the ac magnetic susceptibility for all the doped samples. The temperature dependence of the real part of the ac susceptibility for the doped sample with $x = 0.2$ is shown in Fig. 5(b), and the others are exhibited in Figs. S2–S4. The results show that all the ac susceptibility curves χ' display a peak at the frozen temperature T_f, which is similar to that of the ZFC curve of the dc susceptibility. As the frequency increases, the maximum value of χ' decreases, while the frozen temperature T_f increases, confirming the spin-glass ground state of all the doped samples. In addition, Fig. 5(c) shows the frozen temperature T_f as a function of doping level of S. We can obviously observe that with the doping level increasing, T_f gradually increases from 3.1 K to 5.2 K. The spin glass behavior of the parent compound $Ba_9Co_3Se_{15}$ mainly arises from the magnetic frustration.[9] We speculate that the doping of S enhances the magnetic frustration and then causes the increase of the frozen temperature T_f.

For a 1D conducting chain system, the electron hopping among the chains plays a key role in the transport properties. In $Ba_9Co_3(Se_{1-x}S_x)_{15}$ system, as the content of S doping increases, the inter-chain distance is reduced gradually as shown in Fig. 4. However, the decrease of the inter-chain distance could enhance the 1D conducting characteristic, as will be discussed below. In order to study the fluence of S content on the electronic transport properties, resistivity measurements were performed on the polycrystalline $Ba_9Co_3(Se_{1-x}S_x)_{15}$ ($x = 0$, 0.05, 0.1, 0.15, 0.2) samples. The temperature dependence of resistivity is shown in Fig. 6(a). For all samples, the resistivity increases with decreasing temperature and displays a semiconducting behavior, exhibiting a quasi 1D conducting chain characteristic. Moreover, the resistivity increases more rapidly when the Se atoms are substituted by S. The curves of $\ln\rho$ versus $1/T$ are shown in Fig. 6(b). The straight line in the whole experiment temperature range suggests that the semiconducting behavior can be described based on the Arrhenius law for thermally activated conduction. By using the formula $\rho \propto \exp(\Delta_g/2k_BT)$, where Δ_g is the semiconducting band gap and k_B is the Boltzmann's constant, the resistivity curves are well fitted (shown in Fig. 6(b)) and the band gap could be obtained (shown in Fig. 6(c)). We can observe that as the doping content of S increases, the band gap is gradually enlarged from 0.75 eV for $x = 0$ to 0.86 eV for $x = 0.20$.

Indeed, the increase of band gap in $Ba_9Co_3(Se_{1-x}S_x)_{15}$ as the substitution of Se by S is a typical phenomenon observed in the quasi-one-dimensional conducting chain system, where the transport properties depend on the strength of the electron hopping between the chains.[23,24] Since the S-3p electrons are more localized than Se-4p ones, the replacement of Se by smaller size S should reduce the electron hopping between $CoSe/S_6$ chains and give rise to an increase of the band gap. Therefore, although the interchain distance of Co decreases as the substitution of S into Se sites, the 1D conducting characteristic of $Ba_9Co_3(Se_{1-x}S_x)_{15}$ becomes stronger. Similar phenomena have occurred in $Ba_9Fe_3X_{15}$ (X = S, Se, Te) or $Ba_9Sn_3(Se_xTe_{1-x})_{15}$ series.[10,13,19] Besides chemical dop-

ing, high pressure also provides an effective way to change the inter-chain distance, then enhances the inter-chain electric hopping, and thus changes the 1D conducting chain system to a three-dimensional metal. In this process, some interesting physical properties have been observed like metal to insulator transition in $Ba_9Fe_3Se_{15}$[19] and even possible superconductivity in $Ba_9Fe_3Te_{15}$.[11] $Ba_9Co_3Se_{15}$ possesses the same structure as Ba_9Fe_3Se/Fe_{15} and a 1D conducting chain characteristic, which deserves to be further studied under high pressure.

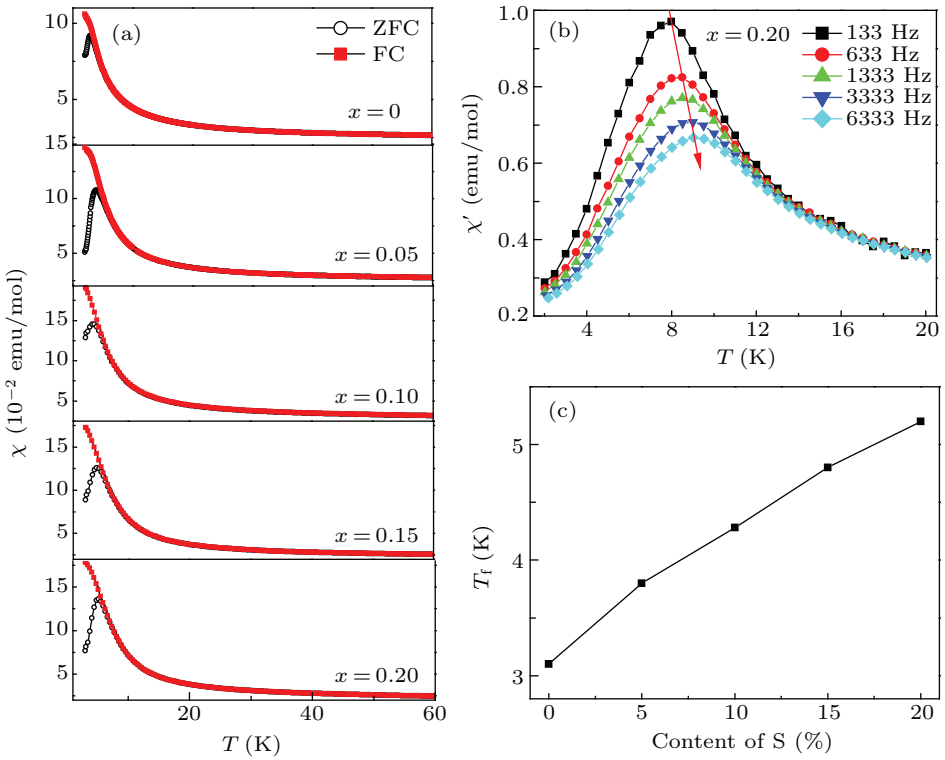


Fig. 5. (a) The magnetic susceptibility as a function of temperature of $Ba_9Co_3(Se_{1-x}S_x)_{15}$ ($x = 0$, 0.05, 0.1, 0.15, 0.2) samples in the range of 2–60 K. (b) The temperature dependence of the real part of ac magnetic susceptibility (χ') for the doped sample with $x = 0.20$ at different frequencies. (c) The frozen temperature T_f of all the samples vs. the doping level of S.

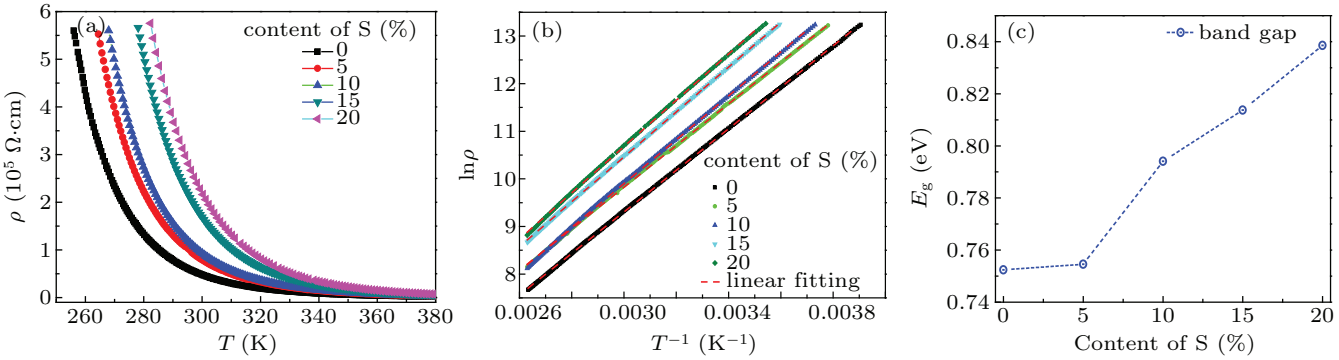


Fig. 6. (a) Temperature dependence of the resistivity for $Ba_9Co_3(Se_{1-x}S_x)_{15}$ ($x = 0$, 0.05, 0.1, 0.15, 0.2); (b) $\ln\rho$ versus $1/T$. The red line is the linear fitting. (c) The S doping dependence of the band gap.

4. Conclusion and perspectives

A series of $Ba_9Co_3(Se_{1-x}S_x)_{15}$ ($x = 0$, 0.05, 0.1, 0.15, 0.2) samples were successfully synthesized under high pressure and high temperature conditions. For all doped samples, the S atoms tend to occupy the site of Se atoms in the $CoSe_6$ octahedron. In physical properties, all the samples are semiconductors and display spin glass behavior, similar to the parent compound $Ba_9Co_3Se_{15}$. The frozen temperature T_f for the doped samples gradually increases with the doping S increasing. Furthermore, the S-3p electrons are more localized than Se-4p ones, which results in the decrease of the electronic hopping among chains. Hence, although the inter-chain instance decreases as the substitution of S increases, the band gap obviously increases.

References

[1] Liu Z Y, Dong Q X, Shan P F, Wang Y Y, Dai J H, Jana R, Chen K Y, Sun J P, Wang B S, Yu X H, Liu G T, Uwatoko Y, Sui Y, Yang H X, Chen G F and Cheng J G 2020 *Chin. Phys. Lett.* **37** 047102

[2] Mu Q G, Ruan B B, Pan B J, Liu T, Yu J, Zhao K, Chen G F and Ren Z A 2017 *Phys. Rev. B* **96** 140504

[3] Tang Z T, Bao J K, Liu Y, Sun Y L, Ablimit A, Zhai H F, Jiang H, Feng C M, Xu Z A and Cao G H 2015 *Phys. Rev. B* **91** 020506

[4] Zhao K, Mu Q G, Ruan B B, Zhou M H, Yang Q S, Liu T, Pan B J, Zhang S, Chen G F and Ren Z A 2020 *Chin. Phys. Lett.* **37** 097401

[5] Mukharjee P K, Ranjith K M, Koo B, Sichelschmidt J, Baenitz M, Skourski Y, Inagaki Y, Furukawa Y, Tsirlin A A and Nath R 2019 *Phys. Rev. B* **100** 144433

[6] Bera A K and Yusuf S M 2012 *Phys. Rev. B* **86** 024408

[7] Hayashida S, Zaharko O, Kurita N, Tanaka H, Hagihala M, Soda M, Itoh S, Uwatoko Y and Masuda T 2018 *Phys. Rev. B* **97** 140405

[8] Matsumoto M, Normand B, Rice T M and Sigrist M 2004 *Phys. Rev. B* **69** 054423

[9] Duan L, Wang X C, Zhang J, Zhao J F, Cao L P, Li W M, Yu R Z, Deng Z and Jin C Q 2020 *Chin. Phys. B* **29** 036102

[10] Zhang J, Duan L, Wang Z, Wang X, Zhao J, Jin M, Li W, Zhang C, Cao L, Deng Z, Hu Z, Agrestini S, Valvidares M, Lin H J, Chen C T, Zhu J and Jin C 2020 *Inorg. Chem.* **59** 5377

[11] Zhang J, Jin M L, Li X, Wang X C, Zhao J F, Liu Y, Duan L, Li W M, Cao L P, Chen B J, Wang L J, Sun F, Wang Y G, Yang L X, Xiao Y M, Deng Z, Feng S M, Jin C Q and Zhu J L 2020 *Chin. Phys. B* **29** 036102

[12] Zhang J, Liu M, Wang X, Zhao K, Duan L, Li W, Zhao J, Cao L, Dai G, Deng Z, Feng S, Zhang S, Liu Q, Yang Y F and Jin C 2018 *J. Phys. Condens. Matter.* **30** 214001

[13] Zhang J, Su R, Wang X, Li W, Zhao J, Deng Z, Zhang S, Feng S, Liu Q, Zhao H, Guan P and Jin C 2017 *Inorg. Chem. Front.* **4** 1337

[14] Duan L, Zhang J, Wang X, Zhao Z, Xiao C, Li X, Hu Z, Zhao J, Li W, Cao L, Dai G, Ren C, He X, Yu R, Liu Q, Tjeng L H, Lin H J, Chen C T and Jin C 2021 *J. Alloys Compds.* **859** 157839

[15] Mermin N D and Wagner H 1966 *Phys. Rev. Lett.* **17** 1133

[16] Jin C Q 2017 *MRS Advances* **2** 2587

[17] Nakamura H, Yamasaki T, Giri S, Imai H, Shiga M, Kojima K, Nishi M, Kakurai K and Metoki N 2000 *J. Phys. Soc. Jpn* **69** 2763

[18] Akrap A, Stevanović V, Herak M, Miljak M, Barišić N, Berger H and Forró L 2008 *Phys. Rev. B* **78** 235111

[19] Zhang J, Komarek A C, Jin M, Wang X, Jia Y, Zhao J, Li W, Hu Z, Peng W, Wang X, Tjeng L H, Deng Z, Yu R, Feng S, Zhang S, Liu M, Yang Y, Lin H, Chen C, Li X and Jin C 2021 *Phys. Rev. Mater.* **5** 054606

[20] Jenks J T H, Rendon-Diaz Miron L E, Cohen S and Steinfink H 1978 *Inorg. Chem.* **17** 1773

[21] C. Q. Jin S A, Wu X J, Yamauchi H and Tanaka S 1994 *Physica C* **223** 238

[22] C. Q. Jin X J W, Laffez P, Tatsuki T, Tamura T, Adachi S, Yamauchi H, Koshizuka N and Tanaka S 1995 *Nature* **375** 301

[23] Gauzzi F L A, Barišić N, Calestani G L, Bolzoni F, Gilioli E, Marezio M, Sanna A, Franchini C and Forr L 2003 *International Journal of Modern Physics B* **17** 3503

[24] Duan L, Zhang J, Wang X, Zhao J, Cao L, Li W, Deng Z, Yu R, Li Z and Jin C 2020 *J. Alloys Compd.* **831** 154697